Journal of
Clinical Medicine

MDPI

Case Report

From Ureteropelvic Junction Obstruction to Giant Hydronephrosis: Molecular Imaging and Multimodal Assessment of Residual Renal Function in a Paediatric Case

Brindusa-Casiana Acsinte [1,2], Irena-Cristina Grierosu [1,3,*], Wael Jalloul [1,3,*], Iuliana-Magdalena Starcea [1,4,5], Maria Adriana Mocanu [1,4], Roxana Alexandra Bogos [1,4], Tudor Ilie Lazaruc [1,4], Madalina Andreea Beldie [1,4,5], Ora Israel [6], Zvi Bar-Sever [7] and Cipriana Stefanescu [1,3]

1 "Grigore T. Popa" University of Medicine and Pharmacy, 700115 Iași, Romania
2 Pediatric Department, "St. Maria" Emergency Children Hospital, 700309 Iași, Romania
3 Nuclear Medicine Laboratory, "St. Spiridon" County Emergency Hospital, 700111 Iași, Romania
4 Department of Pediatric Nephrology, "St. Maria" Emergency Children Hospital, 700309 Iași, Romania
5 Centre for Translational Medicine, Semmelweis University, 1085 Budapest, Hungary
6 Rappaport Faculty of Medicine, Technion Israel Institute of Technology, Haifa 3525433, Israel
7 Department of Nuclear Medicine, Schneider Children's Medical Center, Petah Tikva 4920235, Israel
* Correspondence: irena.raileanu@umfiasi.ro (I.-C.G.); jalloul.wael@umfiasi.ro (W.J.)

Abstract

Giant hydronephrosis is rare and can distort renal architecture, challenging scintigraphic region of interest (ROI) delineation and residual function assessment. Anatomical and molecular imaging can inform decisions between renal preservation and nephrectomy. We report a 13-year-old boy with congenital ureteropelvic junction obstruction and persistent giant hydronephrosis after pyeloplasty in infancy. Assessment combined serial technetium-99m diethylenetriaminepentaacetic acid (^{99m}Tc-DTPA) renography, technetium-99m dimercaptosuccinic acid (^{99m}Tc-DMSA) cortical imaging, single-photon emission computed tomography/computed tomography (SPECT/CT) and CT urography. ^{99m}Tc-DTPA renography showed persistent left-sided tracer retention without evident diuretic washout. ^{99m}Tc-DMSA imaging demonstrated cortical uptake despite marked parenchymal thinning; SPECT/CT localised uptake to residual parenchyma; and CT urography clarified the renal configuration and demonstrated markedly delayed excretion. Initial planar ^{99m}Tc-DMSA processing used left renal ROIs encompassing the enlarged renal outline, while reprocessing used manually delineated cortical ROIs intended to exclude central regions of the dilated collecting system. The two analyses of the same acquisition yielded left/right relative uptake estimates of 70%/30% and 58.72%/41.28%, respectively. Integrated findings contributed to a multidisciplinary decision to preserve the kidney with repeat ureteral stenting. Cortical uptake and relative estimates require interpretation alongside anatomical, drainage and clinical findings; they do not independently establish absolute renal function or recoverability.

Keywords: giant hydronephrosis; ureteropelvic junction obstruction; molecular imaging; ^{99m}Tc-DTPA renography; ^{99m}Tc-DMSA scintigraphy; SPECT/CT; region of interest delineation; renal preservation

Check for updates

Academic Editor: Antonios H. Tzamaloukas

Received: 15 October 2026
Revised: 16 November 2026
Accepted: 23 November 2026
Published: 28 November 2026

Copyright: © 2026 by the authors. Licensee MDPI, Basel, Switzerland. This article is an open access article distributed under the terms and conditions of the Creative Commons Attribution (CC BY) license.

1. Introduction

Congenital ureteropelvic junction obstruction (UPJO) impairs urine passage from the renal pelvis to the ureter and is an important cause of antenatally detected hydronephro-

sis [1]. Its clinical significance lies in the risk of progressive renal dysfunction and the need to identify renal units that may benefit from intervention. Pyeloplasty aims to improve drainage and preserve function, although collecting system dilatation may persist after successful repair [2]. Persistent postoperative hydronephrosis therefore requires integrated anatomical and functional assessment. Giant hydronephrosis represents a rare extreme of collecting system expansion and remains a diagnostic challenge in paediatric patients [3,4]. Marked distortion of the renal outline and severe parenchymal thinning can complicate reassessment and management [3,4].

The degree of parenchymal thinning is clinically relevant, but a thickness measurement alone cannot establish the distribution or functional contribution of the residual tissue. Ultrasonography (US) characterises collecting system dilatation and parenchymal thickness, while renal cortical scintigraphy maps regional tracer uptake and can identify functioning parenchyma in anatomically abnormal kidneys [5,6]. In a profoundly enlarged and distorted renal unit, these modalities provide complementary information about structure and residual cortical function. A relative uptake percentage must be interpreted in relation to both kidneys: it does not independently quantify absolute function or establish functional recoverability [5].

Renal scintigraphy uses radiopharmaceutical behaviour to investigate biological processes in vivo, complementing anatomical imaging with information on renal perfusion, tracer handling and excretion [7]. Diuretic renography with technetium-99m diethylenetriaminepentaacetic acid (^{99m}Tc-DTPA), a glomerular filtration tracer, evaluates differential renal function and tracer clearance from the collecting system under diuretic challenge. Its interpretation depends on renal function, collecting system capacity and compliance, hydration, bladder conditions, the timing of diuretic administration and acquisition methodology [7,8]. Technetium-99m dimercaptosuccinic acid (^{99m}Tc-DMSA) is retained in the renal cortex and demonstrates the spatial distribution of functioning parenchyma [5,9]. Experimental work in megalin/cubilin-deficient mice has demonstrated the contribution of proximal tubular receptor-mediated endocytosis to ^{99m}Tc-DMSA accumulation, providing a biological basis for cortical molecular imaging [10]. Renal perfusion and filtration also influence uptake, linking the scintigraphic signal to several physiological processes [5,10]. Single-photon emission computed tomography/computed tomography (SPECT/CT) can co-localise this signal with anatomical structures. In severe hydronephrosis, relative uptake estimates may be influenced by differences in renal depth, photon attenuation, retained collecting system activity, region-of-interest delineation and background correction [5].

We report the longitudinal multimodal reassessment of a child with congenital UPJO and giant hydronephrosis persisting after pyeloplasty in infancy. Serial ^{99m}Tc-DTPA renography documented persistent left renal tracer retention, while subsequent ^{99m}Tc-DMSA imaging demonstrated cortical uptake despite pronounced parenchymal thinning. The unusual renal configuration complicated anatomical interpretation and relative uptake quantification. This case addresses a specific question: how should residual cortical function be interpreted when renal anatomy is profoundly distorted? Our objective is to illustrate the complementary contributions of serial diuretic renography, planar ^{99m}Tc-DMSA imaging, SPECT/CT and CT urography to anatomical reassessment and kidney-preserving management, with particular attention to the interpretation of cortical tracer uptake and the influence of region of interest delineation on relative uptake estimates.

2. Case Presentation

2.1. Clinical History and Longitudinal Course

A 13-year-old boy with congenital left UPJO was reassessed in 2026 for persistent hydronephrosis following pyeloplasty in infancy. The condition had been detected on

antenatal US at 22 weeks of gestation. Postnatal assessment identified a palpable left flank mass, and US showed marked collecting system dilatation with a thin residual parenchymal rim; the right kidney appeared normal. Intravenous urography demonstrated markedly delayed left contrast excretion, with complete collecting system evacuation reported at 24 h. Left pyeloplasty was performed at six months of age. The postoperative course was complicated by a urinary tract infection caused by multidrug-resistant *Klebsiella* spp., which responded to targeted antibiotic treatment.

Serial ^{99m}Tc-DTPA diuretic renography between 2015 and 2022 consistently demonstrated an accumulation-type left renal curve with persistent tracer retention and no evident washout response to furosemide. US continued to show marked dilatation and a thin parenchymal rim. During this period, the patient remained clinically well, with no documented recurrent urinary tract infections or hypertension. Serum creatinine concentrations ranged from 0.41 to 0.53 mg/dL. Following multidisciplinary review, clinical and imaging surveillance was continued.

Persistent hydronephrosis prompted insertion of a left double-J (JJ) ureteral stent in 2024 to provide internal urinary drainage. The postoperative course was uneventful, but collecting system dilatation persisted after stent removal in March 2025.

At the January 2026 assessment, blood pressure was 100/75 mmHg. US showed a left kidney measuring 14 cm, renal pelvic dilatation of 9.6 cm and a residual parenchymal rim measuring up to 2.5 mm in the mid-renal region. At the March assessment, the patient remained clinically well and afebrile. Serum creatinine was 0.60 mg/dL and serum urea was 33 mg/dL. Using the recorded height of 165 cm, the estimated glomerular filtration rate (eGFR) was retrospectively calculated as 113.6 mL/min/1.73 m^2 with the 2009 bedside Schwartz equation [11]; urinalysis showed no proteinuria, haematuria or pyuria. Given the persistent dilatation and pronounced parenchymal thinning, ^{99m}Tc-DMSA imaging was performed to assess the distribution of residual functioning parenchyma and inform further management. The clinical course and kidney-preserving interventions are summarised in Table 1.

Table 1. Clinical timeline and kidney-preserving interventions.

Time Point/Age	Assessment or Intervention	Key Findings and Management
Antenatal (22 weeks of gestation)	US	Left hydronephrosis detected.
April 2013 (2 months)	Clinical assessment and US	Palpable left flank mass; marked left collecting system dilatation with a thin residual parenchymal rim. Right kidney appeared normal.
20 April 2013 (2 months)	Cystography	Reported as normal.
May 2013 (3 months)	Intravenous urography	Delayed left contrast excretion, with no left ureteral opacification at 3 h. Complete collecting system evacuation reported at 24 h; findings supported the clinical diagnosis of UPJO.
22 August 2013 (6 months)	Left pyeloplasty	Postoperative urinary tract infection caused by multidrug-resistant Klebsiella spp., with a favourable response to targeted antibiotic treatment.
March 2014 (1 year)	US	Persistent left hydronephrosis; residual parenchymal thickness of 3.5–4 mm. Right kidney remained sonographically normal.

Table 1. *Cont.*

Time Point/Age	Assessment or Intervention	Key Findings and Management
18 November 2015 (2 years 9 months)	^{99m}Tc-DTPA diuretic renography	Left accumulation-type curve with persistent tracer retention and no evident washout after furosemide administered at 20 min (F + 20). Right-sided drainage responded to the diuretic.
22 May 2017 (4 years 3 months)	^{99m}Tc-DTPA diuretic renography	Persistent left accumulation-type curve without an evident diuretic washout response (F + 1). Right renal curve appeared normal, with improvement compared with 2015.
9 October 2018 (5 years 8 months)	^{99m}Tc-DTPA diuretic renography	Persistent left tracer retention without evident washout after furosemide (F + 1) or voiding.
August–September 2020 (7 years)	Clinical review and US	Persistent left hydronephrosis with a thin parenchymal rim. Planned renography was deferred during the COVID-19 pandemic; surveillance continued.
11 October 2022 (9 years 8 months)	^{99m}Tc-DTPA diuretic renography; US recorded for October 2022	Left tracer retention persisted after furosemide (F + 1) and voiding. US measurements recorded for that month included a left kidney of 13.5 cm, renal pelvic dilatation of 8 cm and a thin residual parenchymal rim; right kidney measured 8.5 cm.
4 October 2024 (11 years 7 months)	Cystoscopy and left JJ stent insertion	Internal urinary drainage established using a 4 Fr, 20 cm JJ stent. Postoperative course was uneventful.
March 2025 (12 years)	Cystoscopic JJ stent removal and US	Persistent left hydronephrosis, with a reported parenchymal thickness of 9 mm.
28 January 2026 (12 years 11 months)	Clinical reassessment and US	Left kidney measured 14 cm, with renal pelvic dilatation of 9.6 cm and a residual parenchymal rim measuring up to 2.5 mm in the mid-renal region. The right kidney measured 10.4 cm. ^{99m}Tc-DMSA imaging was requested to assess residual functioning parenchyma.
20 March 2026 (13 years 1 month)	Planar ^{99m}Tc-DMSA imaging and SPECT/CT	Cortical tracer uptake was demonstrated within the enlarged, severely distorted left renal unit and anatomically localised to residual parenchymal tissue.
April 2026 (13 years)	CT urography and left JJ stent reinsertion	CT demonstrated giant hydronephrosis of a non-fused left kidney with markedly delayed contrast excretion. A left JJ stent was reinserted.

US: ultrasonography; UPJO: ureteropelvic junction obstruction; JJ: double-J ureteral stent; DTPA: diethylenetriaminepentaacetic acid; DMSA: dimercaptosuccinic acid; CT: computed tomography; SPECT/CT: single-photon emission computed tomography/computed tomography; F + 20 and F + 1: furosemide administered 20 min and 1 min after tracer injection, respectively.

2.2. Imaging Protocols and Quantitative Methods

The imaging assessment comprised serial US, intravenous urography in infancy and postoperative ^{99m}Tc-DTPA diuretic renography, followed by planar ^{99m}Tc-DMSA cortical imaging with SPECT/CT and contrast-enhanced CT urography in 2026. These investigations provided complementary information on renal and collecting system morphology, tracer uptake and drainage, and the anatomical distribution of residual cortical uptake. Quantitative assessment included the reported ^{99m}Tc-DTPA-derived functional estimates and comparison of the initial and reprocessed planar ^{99m}Tc-DMSA relative uptake estimates

obtained using different renal regions of interest (ROIs). Radiopharmaceutical activities were selected according to body weight using the laboratory's paediatric protocol, guided by the European Association of Nuclear Medicine (EANM) recommendations [5,8].

2.2.1. Renal Ultrasonography

Serial US assessed renal dimensions, collecting system dilatation and residual parenchymal thickness throughout follow-up.

2.2.2. Intravenous Urography

Intravenous urography was performed in infancy, with delayed assessment at 3 and 24 h after contrast administration.

2.2.3. ^{99m}Tc-DTPA Diuretic Renography

Serial diuretic renography was performed with ^{99m}Tc-DTPA. Imaging used a Siemens E.CAM Signature Series dual-detector gamma camera. Recorded body weights and reported tracer activities were 15 kg and 74 MBq (2015), 18 kg and 88 MBq (2017), 21 kg and 103.6 MBq (2018), and 36 kg and 144.3 MBq (2022).

Furosemide was administered 20 min after tracer injection in 2015 (F + 20) and at 1 min in 2017, 2018 and 2022 (F + 1). This change reflected a revision of the laboratory's routine protocol following discussions with the collaborating paediatric nephrology team. Prescribed doses recorded on the request forms were 7.5 mg, 9 mg and 10 mg for 2015, 2017 and 2018, respectively; the 2022 report documented intravenous administration of 18 mg.

All four examinations included dynamic acquisition beginning immediately after intravenous tracer injection and static images obtained before and after voiding. Renal time–activity curves were interpreted alongside the dynamic and static images to assess tracer uptake and drainage.

Differential renal function (DRF) and scintigraphic estimates of glomerular filtration rate (GFR) were obtained from the primary reports and processing outputs. The examinations' processing used the Gates method, with separate renal and background ROIs and the software's "Standard" renal depth method. The scintigraphic GFR estimates were normalised by the processing software to a body surface area of 1.73 m^2 and are reported in mL/min/1.73 m^2. Longitudinal comparisons are descriptive.

2.2.4. ^{99m}Tc-DMSA Renal Cortical Scintigraphy and SPECT/CT

The examination was performed using a GE Optima NM/CT 870DR system after intravenous administration of 118.4 MBq at a recorded body weight of 71 kg. Planar acquisition began 2.5 h after injection and included anterior, posterior, bilateral anterior oblique and bilateral posterior oblique projections, followed by SPECT/CT. Relative uptake estimates were derived from planar images. SPECT/CT with a low-dose CT component covering the abdomen was performed to clarify the anatomical distribution of cortical tracer uptake within the markedly enlarged and distorted left renal unit. The recorded dose–length product (DLP) for the CT component was 170 mGy·cm.

Both the initial and reprocessed relative renal uptake estimates were calculated from background-corrected anterior and posterior planar counts using the geometric mean method implemented in the system's processing software. No additional renal depth or attenuation correction was applied. The initial left renal ROIs encompassed the enlarged renal outline. Reprocessing used manually delineated cortical ROIs intended to exclude central collecting system regions. The background correction method and all other processing settings remained unchanged between analyses; only the renal ROI contours were modified. The initial and reprocessed estimates are reported separately as a comparison of two ROI

strategies applied to the same planar acquisition. Neither estimate was independently validated.

2.2.5. CT Urography

CT urography was performed on 16 April 2026 using a paediatric protocol to characterise the severely distorted renal and collecting system anatomy before consideration of repeat pyeloplasty. Four diagnostic acquisitions were confirmed as performed: unenhanced, arterial, venous and a delayed acquisition at 15 min. Tube voltage was 110 kV for the unenhanced acquisition and 100 kV for the contrast-enhanced acquisitions; effective tube current–time products ranged from 95 to 100 mAs. Acquisition-specific volume computed tomography dose index (CTDIvol) values ranged from 5.30 to 6.69 mGy, referenced to a 32 cm phantom. The cumulative DLP attributable to the performed acquisitions was approximately 921 mGy·cm. This value should be interpreted in the context of the patient's body weight of 71 kg.

2.3. Multimodal Imaging Findings

Serial US documented persistent marked left collecting system dilatation and a thin residual parenchymal rim. The right kidney remained sonographically normal.

Serial ^{99m}Tc-DTPA renography between 2015 and 2022 demonstrated an accumulation-type left renal time–activity curve and persistent tracer retention without an evident washout response to furosemide. Left-sided retention also persisted after voiding in the 2018 and 2022 examinations. In 2015, right-sided collecting system retention responded to furosemide; right-sided tracer washout was also observed in subsequent examinations. Reported left DRF values were 13.9%, 36.7%, 38.2% and 38.1% in 2015, 2017, 2018 and 2022, respectively. The corresponding reported normalised total scintigraphic GFR estimates were 43, 67.6, 58 and 73.3 mL/min/1.73 m^2, respectively. The interpreting reports noted uncertainty in functional quantification of the markedly enlarged left renal unit (Figure 1).

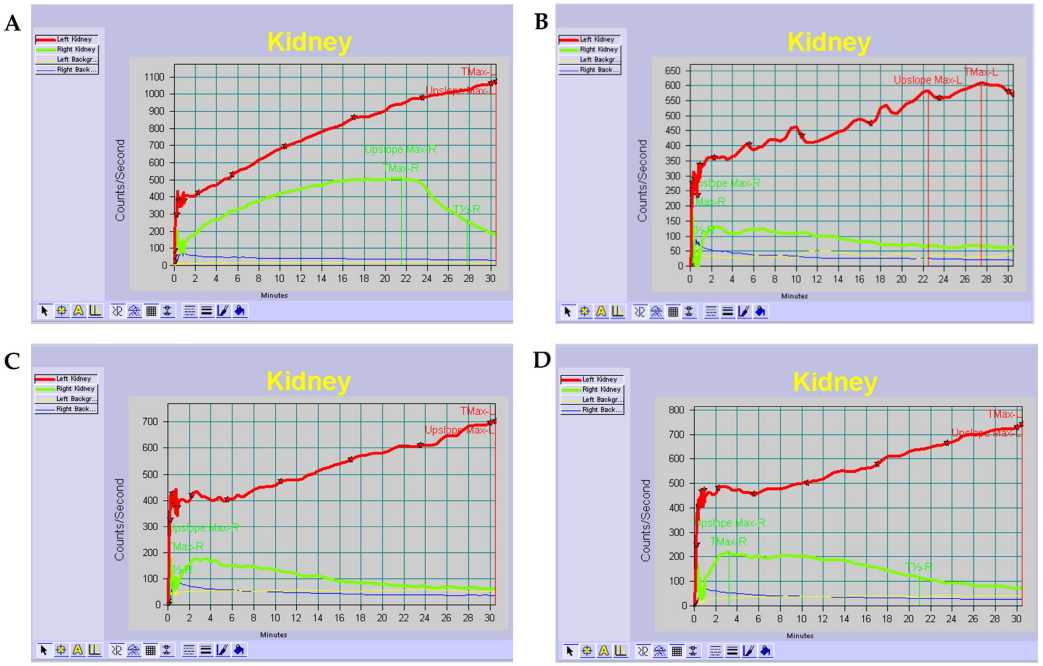


Figure 1. Serial ^{99m}Tc-DTPA diuretic renography demonstrating persistent left-sided tracer retention. Renal time–activity curves from postoperative examinations performed on (**A**) 18 November 2015, (**B**) 22 May 2017, (**C**) 9 October 2018 and (**D**) 11 October 2022. Furosemide was administered 20 min after tracer injection in panel (**A**) (F + 20) and at 1 min in panels (**B**–**D**) (F + 1). The left renal

curves (red) show an accumulation-type pattern without an evident post-diuretic washout response throughout follow-up. The right renal curves (green) show delayed washout following furosemide in panel (**A**) and an earlier peak followed by declining activity in panels (**B**–**D**). Yellow and blue lines represent the left and right background curves, respectively.

Planar ^{99m}Tc-DMSA scintigraphy in March 2026 demonstrated an enlarged left renal unit with an irregular, lobulated distribution of cortical tracer uptake and multiple distinguishable uptake foci. Cortical uptake remained visible despite the pronounced parenchymal thinning reported on US. This unusual pattern initially raised the possibility of a fused renal configuration and prompted further anatomical assessment. The right kidney showed homogeneous cortical uptake (Figure 2).

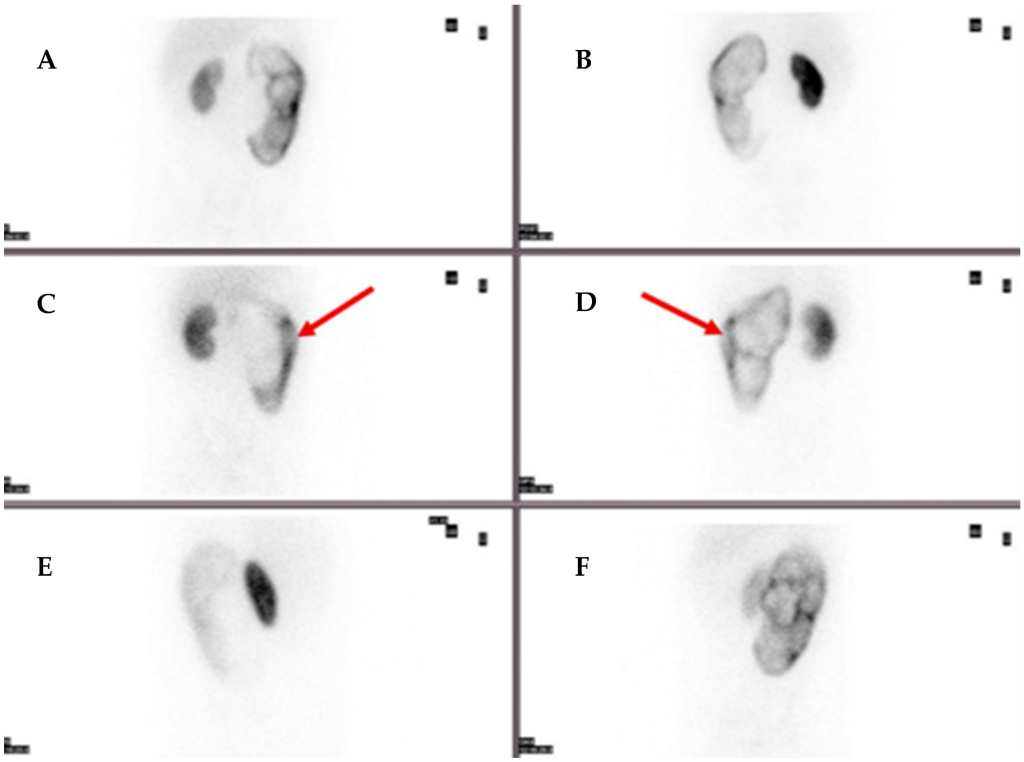


Figure 2. Planar ^{99m}Tc-DMSA renal cortical scintigraphy. (**A**) Anterior; (**B**) posterior; (**C**) right anterior oblique; (**D**) left posterior oblique; (**E**) right posterior oblique; and (**F**) left anterior oblique views. Red arrows in panels (**C**,**D**) indicate cortical tracer uptake in the enlarged left kidney.

SPECT/CT localised the left-sided uptake to the thin, irregular residual parenchymal rim surrounding the markedly dilated collecting system. The collecting system cavities were relatively photopenic compared with the surrounding cortical activity. The left renal unit measured 22.3 × 6.7 × 10 cm in the craniocaudal, anteroposterior and transverse dimensions, respectively (Figures 3 and 4).

CT urography in April 2026 characterised the abnormality as giant hydronephrosis of a non-fused left kidney in its expected anatomical position. Reported renal dimensions were 20.37 × 9.87 cm. The renal pelvis measured 8.44 × 7.12 cm in the anteroposterior and transverse dimensions, respectively, with peripheral displacement of the calyces. Residual parenchymal thickness varied, reaching a reported maximum of 5 mm in the mid-renal region. Left-sided contrast excretion was markedly delayed, and the left ureter was not opacified on excretory or delayed images. The right kidney showed preserved morphology and contrast excretion (Figures 5 and 6).

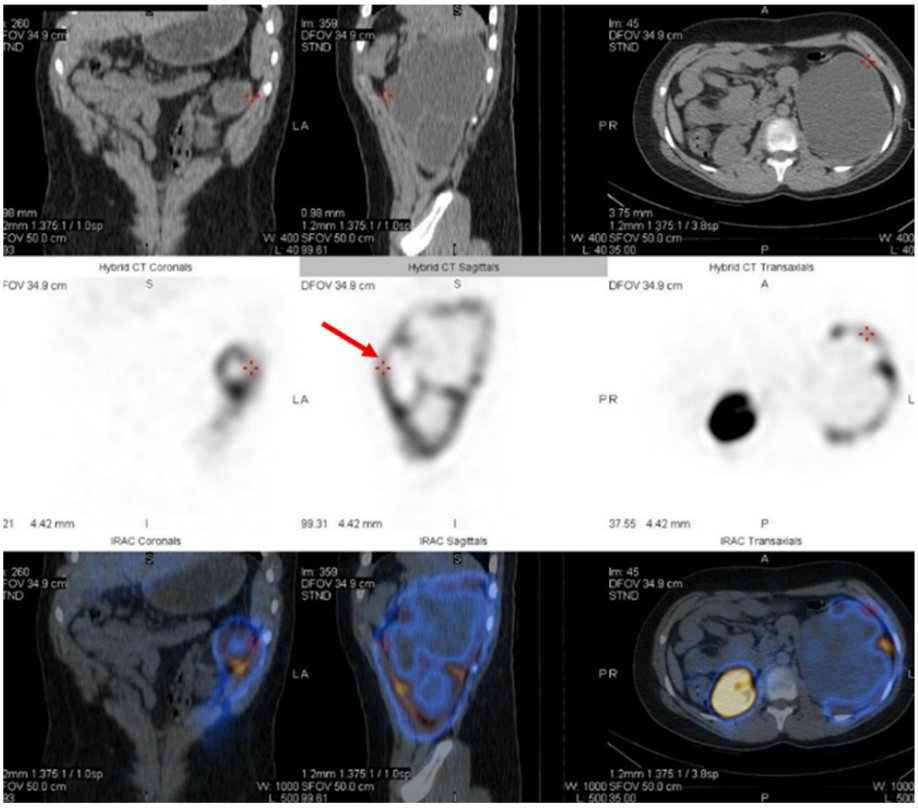


Figure 3. Multiplanar ^{99m}Tc-DMSA SPECT/CT images. Columns show coronal (left), sagittal (centre) and axial (right) views. Rows show low-dose CT (top), SPECT (middle) and fused SPECT/CT (bottom) images. The red arrow indicates tracer uptake in the residual left renal parenchyma.

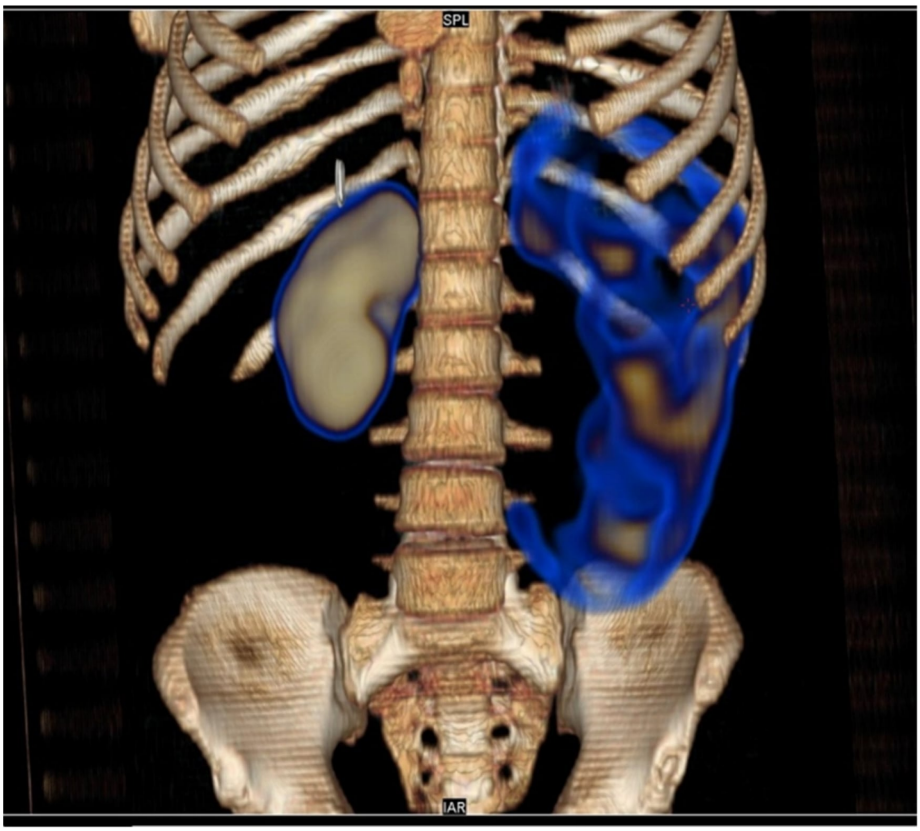


Figure 4. Three-dimensional rendering of ^{99m}Tc-DMSA SPECT/CT.

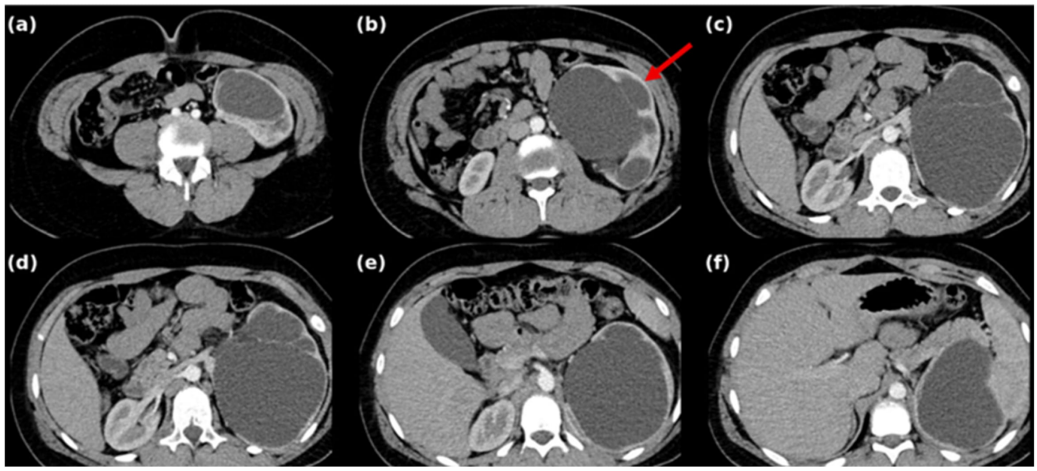


Figure 5. Axial CT images of giant left hydronephrosis. (**a**–**f**) Contrast-enhanced axial sections displayed in caudocranial order. The red arrow in (**b**) indicates the thin residual parenchymal rim surrounding the markedly dilated left collecting system.

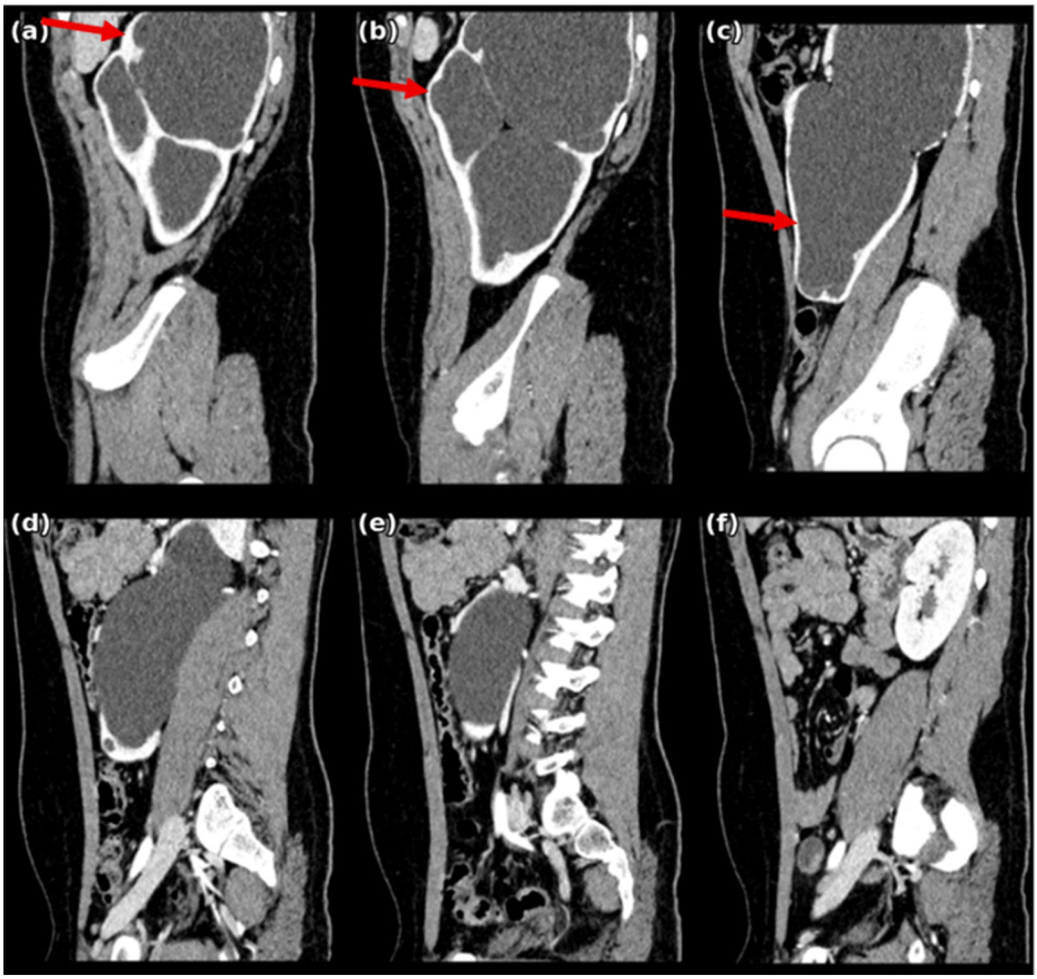


Figure 6. Sagittal CT images of giant left hydronephrosis. (**a**–**e**) Contrast-enhanced sagittal sections through the left renal unit. (**f**) Sagittal section through the right kidney. Red arrows in (**a**–**c**) indicate the thin residual parenchymal rim surrounding the dilated left collecting system.

The initial planar ^{99m}Tc-DMSA ROI analysis, including the entire kidneys, yielded relative uptake estimates of 70% for the left renal unit and 30% for the right kidney. Re-

processing of the same examination using manually delineated cortical ROIs intended to exclude central collecting system regions yielded estimates of 58.72% and 41.28%, respectively. The left relative uptake estimate differed by 11.28 percentage points between the two analyses of the same examination (Figure 7).

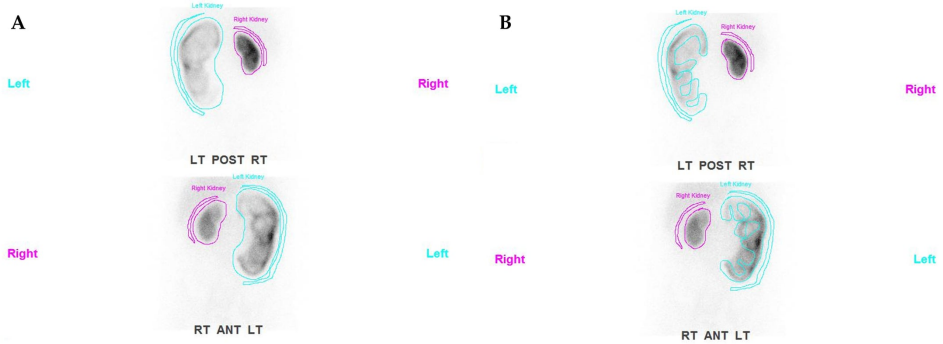


Figure 7. Comparison of ROI delineation in planar ^{99m}Tc-DMSA processing. (**A**) Initial analysis with left renal ROIs encompassing the entire enlarged renal outline (left/right relative uptake: 70%/30%). (**B**) Manual cortical ROI reprocessing, intended to exclude central regions of the dilated left collecting system (58.72%/41.28%). Posterior views are shown above and anterior views below. Cyan and magenta contours identify the left and right renal and background ROIs, respectively. Both analyses derive from the same examination.

Table 2 summarises the reported ^{99m}Tc-DTPA-derived functional estimates and drainage findings alongside the initial and reprocessed ^{99m}Tc-DMSA relative uptake estimates.

Table 2. ^{99m}Tc-DTPA renographic functional estimates and drainage findings, and initial and reprocessed ^{99m}Tc-DMSA relative uptake estimates.

A. ^{99m}Tc-DTPA Diuretic Renography				
Date	**Left DRF (%)**	**Right DRF (%)**	**Normalised Total GFR (mL/min/1.73 m^2)**	**Left-Sided Drainage**
18 November 2015	13.9	86.1	43	Accumulation-type curve; no evident washout after furosemide (F + 20).
22 May 2017	36.7	63.3	67.6	Accumulation-type curve; no evident washout after furosemide (F + 1).
9 October 2018	38.2	61.8	58	Accumulation-type curve; persistent retention after furosemide (F + 1) and voiding.
11 October 2022	38.1	61.9	73.3	Accumulation-type curve; persistent retention after furosemide (F + 1) and voiding.
B. ^{99m}Tc-DMSA scintigraphy in March 2026				
ROI analysis			**Left relative uptake (%)**	**Right relative uptake (%)**
Initial renal outline ROI analysis, including the entire kidneys			70	30
Manual cortical ROI reprocessing, intended to exclude the dilated collecting system			58.72	41.28

DTPA: diethylenetriaminepentaacetic acid; DMSA: dimercaptosuccinic acid; DRF: differential renal function; GFR: glomerular filtration rate; ROI: region of interest; F + 20 and F + 1: furosemide administered 20 min and 1 min after tracer injection, respectively.

2.4. Clinical Decision and Follow-Up

During multidisciplinary reassessment in 2026, kidney-preserving management was maintained, and nephrectomy was deferred. Repeat pyeloplasty was among the reconstructive options considered, and CT urography was obtained to support anatomical assessment before further surgical planning. The decision integrated the clinically stable course with persistent left tracer retention on ^{99m}Tc-DTPA, residual cortical uptake on ^{99m}Tc-DMSA and the clarified renal anatomy. The family had previously expressed a preference for renal preservation during diagnostic reassessment. A second opinion from paediatric nephrology specialists at a tertiary referral centre supported the proposed strategy.

The earlier selection of JJ stenting over percutaneous nephrostomy in 2024 reflected the absence of acute infection and a preference for internal drainage in an active child. A left JJ stent was reinserted on the day of CT urography to provide internal urinary drainage, with radiographic confirmation of correct positioning. The JJ stent was removed on 16 June 2026, approximately two months after reinsertion. The clinical course was reported as favourable.

The family was counselled about the potential risk of renal injury following abdominal or flank trauma in the presence of the markedly enlarged hydronephrotic kidney.

3. Discussion

This case illustrates the integration of dynamic and cortical renal scintigraphy with anatomical imaging during long-term follow-up after pyeloplasty for congenital UPJO. Serial ^{99m}Tc-DTPA examinations documented abnormal left-sided drainage, and the later ^{99m}Tc-DMSA study demonstrated residual cortical uptake within a markedly thinned renal unit. Serial US documented collecting system enlargement and parenchymal thinning, while SPECT/CT and CT urography clarified the anatomy of giant hydronephrosis. The clinical and methodological contribution is to interpret drainage, cortical tracer handling and the uncertainty of relative uptake estimates together when considering renal preservation.

3.1. Congenital UPJO and Obstructive Parenchymal Injury

Congenital UPJO can involve parenchymal injury beyond collecting system dilatation. In children with congenital obstructive nephropathy, Grandaliano et al. demonstrated increased tubulointerstitial gene expression of monocyte chemoattractant protein-1 (MCP-1), associated with monocyte infiltration, and reduced epidermal growth factor (EGF) gene expression, associated with tubular damage [12]. These observations provide a biological link between obstruction, inflammatory recruitment and altered tubular trophic signalling. Biopsy studies have also described tubular atrophy or simplification, interstitial fibrosis and glomerular abnormalities, some of which may reflect parenchymal maldevelopment [13]. Both developmental abnormalities and acquired injury may therefore contribute to the parenchymal changes.

In our patient, antenatal hydronephrosis, persistent drainage abnormalities on serial ^{99m}Tc-DTPA examinations and marked parenchymal thinning are compatible with longstanding obstructive parenchymal injury. The inflammatory and fibrotic mechanisms described in the literature provide a biological context for these findings, although their presence and extent were not established histologically or molecularly in this case. Persistent dilatation after pyeloplasty also does not independently establish recurrent obstruction, since hydronephrosis may remain after successful repair [2]. Its clinical significance must be interpreted alongside tracer transit, post-diuretic drainage and the clinical course.

3.2. Biological Basis of ^{99m}Tc-DTPA and ^{99m}Tc-DMSA Imaging

Molecular imaging characterises biological processes at molecular and cellular levels in living systems [14]. Renal radiopharmaceuticals provide complementary information

on tracer delivery, renal handling and excretion [7]. ^{99m}Tc-DTPA undergoes glomerular filtration, and dynamic acquisition follows renal uptake and subsequent urinary clearance, allowing for estimation of differential functional contribution and evaluation of drainage under diuretic challenge [8]. In this case, ^{99m}Tc-DTPA provided physiological assessment of filtration and drainage, while the molecular imaging perspective concerns the cellular processes underlying ^{99m}Tc-DMSA cortical retention [10,14].

^{99m}Tc-DMSA cortical retention reflects a different aspect of renal tracer handling. Experimental work in megalin/cubilin-deficient mice supports receptor-mediated proximal tubular endocytosis as an important determinant of ^{99m}Tc-DMSA accumulation, with a proposed pathway involving a filtered ^{99m}Tc-DMSA–α1-microglobulin complex [10]. Human observations in Dent disease and Lowe syndrome, in which ^{99m}Tc-DMSA uptake was markedly reduced despite sometimes preserved creatinine clearance, further support an association between cortical accumulation and proximal tubular handling [15]. These findings explain why cortical uptake and glomerular filtration need not change in parallel.

In our patient, the ^{99m}Tc-DTPA studies provided the longitudinal dynamic assessment, while the later ^{99m}Tc-DMSA examination mapped residual cortical uptake despite pronounced thinning. This combination connects glomerular tracer handling and drainage with cortical tracer retention in the assessment of the same renal unit. The ^{99m}Tc-DMSA signal also depends on tracer delivery, renal handling and acquisition conditions [5,10]; it does not measure megalin/cubilin expression, histological fibrosis or functional reserve. Thus, the patient-specific observation is demonstrable cortical uptake within residual parenchyma, rather than evidence of a particular molecular pathway being preserved or a prediction of functional recovery.

3.3. Quantification Challenges in Giant Hydronephrosis

Severe collecting system expansion complicates both dynamic and cortical scintigraphic quantification. In renography, estimation of DRF requires assessment of early parenchymal activity with background correction, whereas drainage curves require ROIs covering the dilated collecting system [8]. Thus, ROI definition must follow the parameter being assessed.

The reported increase in left ^{99m}Tc-DTPA DRF from 13.9% in 2015 to approximately 37–38% from 2017 onward requires cautious interpretation. The transition from F + 20 to F + 1 and potential variation in renal and background ROI delineation may affect longitudinal comparability; consistent acquisition and processing are recommended for serial assessment [8]. The available data do not establish whether the increase reflects true functional change, methodological variation or a combination of both.

An additional interpretative challenge was the numerical discordance between the left DRF of 38.1% reported on the 2022 ^{99m}Tc-DTPA renogram and the 2026 planar ^{99m}Tc-DMSA relative uptake estimates of 70% initially and 58.72% after cortical ROI reprocessing. These percentages describe different tracer processes: ^{99m}Tc-DTPA-derived DRF is based on early uptake of a glomerular filtration tracer, whereas ^{99m}Tc-DMSA relative uptake reflects delayed cortical retention influenced by proximal tubular handling [5,8,10]. The examinations were performed at different stages of follow-up, with intervening JJ stent insertion and removal. The recorded body weight increased from 36 kg at the 2022 examination to 71 kg at the 2026 examination. Changes in body habitus during growth and weight gain may influence renal depth and photon attenuation when comparing examinations, although their contribution to the scintigraphic estimates cannot be quantified from weight alone [5]. The cause of this discordance cannot be established from the available data, and the higher ^{99m}Tc-DMSA percentage cannot be interpreted as evidence of functional recovery or superior accuracy.

The central methodological finding was the change in left ^{99m}Tc-DMSA relative uptake from 70% with the initial renal outline ROIs to 58.72% with manually delineated cortical ROIs

intended to exclude central collecting system regions. The corresponding right estimates were 30% and 41.28%. The difference between the percentages arose from two analyses of one acquisition and cannot represent an interval biological change. Neither estimate was independently validated as the true relative cortical contribution.

For planar ^{99m}Tc-DMSA analysis, relative uptake expresses each kidney's background-corrected activity as a proportion of the combined renal activity. A larger ROI does not, by itself, prove overestimation: an area containing only background activity should make little net contribution after appropriate correction. Changes in contouring may nevertheless alter the inclusion of non-cortical activity, background counts and area-dependent background subtraction. Renal depth and photon attenuation can introduce further asymmetry [5]. A thin but extensive cortical rim may also retain measurable activity; local thickness alone cannot predict its total contribution to the planar signal. The relatively photopenic collecting system cavities on SPECT/CT support cortical localisation but do not quantify any contribution of retained urinary activity to the planar counts.

The ^{99m}Tc-DMSA guideline recommends whole-kidney ROIs, permits exclusion of the renal pelvis and requires appropriate background subtraction. For severe hydronephrosis, the guideline recommends calculation of relative uptake using the geometric mean of anterior and posterior counts to reduce bias from unequal renal depth; collecting system retention and attenuation remain relevant sources of error [5]. Restricting an ROI to the apparent cortex does not correct all attenuation or depth effects and risks omitting functioning tissue if the thin rim is incompletely outlined. On planar images, excluding central collecting system regions may also remove superimposed cortical activity.

With the geometric mean calculation, background correction method and all other processing settings held constant, the observed difference reflects the effect of changing the renal ROI contours within the same acquisition. This demonstrates the sensitivity of relative uptake estimates to ROI delineation in severely distorted anatomy, without establishing which estimate more accurately represents the relative cortical contribution. Nam et al. proposed a modified ^{99m}Tc-DTPA-derived DRF index normalised to renal cross-sectional area [16]. This illustrates how changing the definition of a functional index changes its interpretation without validating cortical ROI processing of ^{99m}Tc-DMSA. The paired estimates in our case make a quantification discrepancy visible before either percentage is used to support a management decision.

3.4. Complementary Roles of Multimodal Imaging

The modalities addressed distinct clinical questions. Serial US described collecting system dilatation and the residual parenchymal rim, while ^{99m}Tc-DTPA provided longitudinal information on tracer uptake and drainage. Persistent left retention after furosemide, including post-void retention documented in 2018 and 2022, reinforced the evidence of impaired emptying. However, washout is affected by renal function, collecting system capacity and compliance, hydration and bladder conditions; absent washout should not be used alone to determine the severity of mechanical obstruction [8].

The 2026 ^{99m}Tc-DMSA examination addressed the complementary question of residual cortical tracer uptake. SPECT/CT related the irregular uptake pattern to the distorted parenchymal rim, and CT urography subsequently confirmed giant collecting system expansion within the left renal unit, with delayed contrast excretion. Combined drainage and cortical imaging has also been useful in selected children with complex congenital renal anatomy, as illustrated by Filippi et al. [17]. In our patient, integrating the ^{99m}Tc-DTPA history with cortical and anatomical imaging clarified the drainage defect, residual uptake distribution and severe anatomical distortion.

The 14 cm left renal measurement reported on US in January 2026 and the 20–22 cm measurements on subsequent SPECT/CT and CT urography should not be assumed to be directly comparable. In this severely distorted renal unit, differences in measurement plane, orientation and delineation of the expanded collecting system may have contributed to the discrepancy. The examinations were performed at different time points, and identical anatomical endpoints cannot be confirmed from the reported measurements. The numerical difference alone therefore does not establish interval renal growth.

US remains the preferred modality for routine anatomical follow-up in children, while magnetic resonance urography (MRU), including functional MRU (fMRU), can provide additional anatomical and functional information without ionising radiation [18]. Pensabene et al. reviewed ultrasound-based approaches to the diagnosis and follow-up of primary vesicoureteral reflux, illustrating the broader role of non-ionising imaging in paediatric urology [19].

In this patient, CT urography addressed the complex renal and collecting system anatomy before consideration of repeat pyeloplasty when MRU was unavailable. Radiation protection measures included body weight-based selection of radiopharmaceutical activities and the use of paediatric CT protocols, with hybrid CT coverage restricted to the abdomen.

3.5. Implications for Kidney-Preserving Management

The decision to continue renal preservation and defer nephrectomy integrated the previously asymptomatic course, absence of reported recurrent infections or hypertension, earlier reports of preserved overall renal function and the family's preference for preservation during diagnostic reassessment. The history of impaired drainage on ^{99m}Tc-DTPA was considered alongside residual cortical uptake on ^{99m}Tc-DMSA and the anatomical findings. Internal JJ drainage was selected within this individual clinical context. Kidney-preserving procedures described for giant hydronephrosis include reduction pyeloplasty and adjunctive nephroplication or nephropexy in selected patients [3,20]. Sarhan et al. reported functional improvement after pyeloplasty in some children with low renographic DRF but excluded patients with previous renal or ureteric surgery [21]. These findings cannot directly predict recoverability in this patient's left kidney, which had undergone pyeloplasty in infancy. Similarly, changes in reported parenchymal thickness after drainage cannot establish regeneration or functional improvement without comparable measurement planes and assessment conditions.

Temporary percutaneous nephrostomy (PCN) represents a complementary diagnostic option when uncertainty about an obstructed kidney's residual function could influence further management. It permits decompression and separate urine collection for assessment of ipsilateral urine output and creatinine clearance, using timed collection with concurrent serum creatinine measurement [22]. Urinary specific gravity or osmolality and electrolyte excretion can additionally inform assessment of concentrating ability and tubular handling. Interpretation requires attention to post-decompression stabilisation, completeness of collection for clearance calculations and tubular creatinine secretion [22]. In a cohort of children with UPJO and DRF <10%, temporary drainage through a JJ stent or PCN followed by functional reassessment was used to guide subsequent management [23]. These findings cannot directly predict recoverability in this patient's previously operated left kidney. In our patient, internal JJ drainage was selected in the clinical context described above. PCN-based assessment could have provided complementary information about left renal function if uncertainty persisted before further reconstruction or nephrectomy, although it would not directly validate either ^{99m}Tc-DMSA relative uptake estimate.

In a paediatric UPJO series, Menon et al. proposed considering nephrectomy when absent or minimal isotope uptake coexisted with absent parenchyma, pyonephrosis, hy-

pertension or minimal urine output through PCN [24]. For this patient, any future reconsideration would require reliable reassessment of the left kidney's contribution and the feasibility of further reconstruction. Recurrent infection, persistent pain, hypertension or convincing functional deterioration would warrant renewed multidisciplinary assessment without constituting automatic indications for nephrectomy.

The distinction between demonstrable cortical uptake and recoverable function is central to management. Residual uptake can inform consideration of preservation, while the benefit of drainage requires assessment through subsequent clinical and functional follow-up. Such evaluation should integrate symptoms, blood pressure, renal biochemistry, urinary findings and imaging obtained under comparable conditions [8,21]. The creatinine-based eGFR estimates overall filtration and cannot independently establish the affected kidney's functional contribution or recoverability. The documented intervention represents a preservation strategy whose functional benefit remains to be established.

3.6. Strengths and Limitations

The principal strengths are follow-up from antenatal detection into adolescence, serial ^{99m}Tc-DTPA documentation of tracer uptake and drainage, and later integration of ^{99m}Tc-DMSA cortical imaging with SPECT/CT and CT urography. This combination documents the course of drainage abnormalities and the anatomical location of residual cortical uptake in one severely distorted renal unit. The same ^{99m}Tc-DMSA acquisition was analysed using two ROI strategies, allowing for a processing-related discrepancy to be described without an intervening biological change. The retrospective single-case design, however, limits generalisation and quantitative validation.

Serial diuretic renography used ^{99m}Tc-DTPA because technetium-99m mercaptoacetyltriglycine (^{99m}Tc-MAG3) was unavailable owing to a nationwide shortage at the time of the examinations. The paediatric guideline accepts the use of ^{99m}Tc-DTPA when tubular agents are unavailable, but ^{99m}Tc-MAG3's higher extraction generally offers better renal-to-background contrast in severely dilated systems or impaired renal function [8]. The magnitude of any tracer-related effect in this patient cannot be determined without a paired comparison.

CT urography was performed in place of MRU because the hospital's magnetic resonance scanner was temporarily out of service owing to a technical malfunction. This involved additional ionising radiation and prevented complementary assessment with fMRU, which can combine anatomical characterisation, functional evaluation and drainage assessment without ionising radiation [18].

4. Conclusions

In this case, giant hydronephrosis with profound anatomical distortion and cortical thinning coexisted with demonstrable residual ^{99m}Tc-DMSA cortical uptake. Serial ^{99m}Tc-DTPA renography, ^{99m}Tc-DMSA imaging with SPECT/CT and CT urography provided complementary information on drainage, cortical tracer distribution and renal configuration. These findings contributed to a multidisciplinary decision to maintain renal preservation.

Discordance between ^{99m}Tc-DTPA-derived DRF and ^{99m}Tc-DMSA relative uptake, together with the difference between two ROI analyses of the same ^{99m}Tc-DMSA acquisition, emphasises the need to interpret percentages according to tracer biology, examination timing, processing methodology and anatomical context. Neither ^{99m}Tc-DMSA estimate was independently validated. Residual cortical uptake alone does not establish adequate absolute renal function, functional reserve or recoverability; comparable clinical and functional follow-up is needed to assess the benefit of urinary drainage.

Author Contributions: Conceptualisation, B.-C.A. and I.-C.G.; Methodology, I.-C.G., C.S., O.I. and Z.B.-S.; Investigation, B.-C.A., I.-C.G., I.-M.S., M.A.M., R.A.B., T.I.L. and M.A.B.; Resources, I.-C.G. and I.-M.S.; Data Curation, B.-C.A. and I.-C.G.; Writing—Original Draft Preparation, B.-C.A. and W.J.; Writing—Review and Editing, W.J., I.-C.G., I.-M.S., M.A.M., R.A.B., T.I.L., M.A.B., O.I., Z.B.-S. and C.S.; Visualisation, W.J., I.-C.G. and B.-C.A.; Supervision, C.S. and I.-C.G.; Project Administration, I.-C.G. All authors have read and agreed to the published version of the manuscript.

Funding: This research received no external funding.

Institutional Review Board Statement: Ethical approval for this case report was obtained from the Ethics Committee of "Sf. Maria" Children's Emergency Clinical Hospital, Iasi, Romania (approval No. 28716, dated 1 September 2026). The report was prepared in accordance with the Declaration of Helsinki and was based on de-identified clinical, laboratory and imaging data collected during routine patient care.

Informed Consent Statement: Written informed consent was obtained from the patient's legal guardian for publication of this case report and the accompanying images.

Data Availability Statement: The data supporting the conclusions of this article will be made available by the corresponding author upon reasonable request.

Acknowledgments: The authors would like to express their sincere gratitude to Radu Valentin Russu, Department of Paediatric Nephrology, "St. Maria" Children's Emergency Hospital, Iasi, Romania for his dedicated care and long-term follow-up of the patient presented in this case report, as well as for his valuable clinical collaboration and support. The authors would also like to express their sincere gratitude to Gabriela Lăcrămioara Buhuș, Department of Radiology and Medical Imaging for her valuable contribution to the imaging evaluation of this complex case and for her professional expertise, which supported the diagnostic and therapeutic decision-making process. The authors used Grammarly AI (v1.2.316.2014) to assist with manuscript drafting and language editing. All content was reviewed by the authors, who take full responsibility for the final manuscript.

Conflicts of Interest: The authors declare no conflicts of interest.

Abbreviations

The following abbreviations are used in this manuscript:

AI	Artificial intelligence
COVID-19	Coronavirus disease 2019
CT	Computed tomography
CTDIvol	Volume computed tomography dose index
DLP	Dose–length product
DMSA	Dimercaptosuccinic acid
DRF	Differential renal function
DTPA	Diethylenetriaminepentaacetic acid
EANM	European Association of Nuclear Medicine
eGFR	Estimated glomerular filtration rate
EGF	Epidermal growth factor
F + 1	Furosemide administered 1 min after tracer injection
F + 20	Furosemide administered 20 min after tracer injection
fMRU	Functional magnetic resonance urography
GFR	Glomerular filtration rate
JJ	Double-J ureteral stent
MAG3	Mercaptoacetyltriglycine
MCP-1	Monocyte chemoattractant protein-1
MRU	Magnetic resonance urography
PCN	Percutaneous nephrostomy
ROI	Region of interest
SPECT	Single-photon emission computed tomography
SPECT/CT	Single-photon emission computed tomography/computed tomography
UPJO	Ureteropelvic junction obstruction
US	Ultrasonography

References

1. Nguyen, H.T.; Herndon, C.D.A.; Cooper, C.; Gatti, J.; Kirsch, A.; Kokorowski, P.; Lee, R.; Perez-Brayfield, M.; Metcalfe, P.; Yerkes, E.; et al. The Society for Fetal Urology Consensus Statement on the Evaluation and Management of Antenatal Hydronephrosis. *J. Pediatr. Urol.* **2010**, *6*, 212–231. [CrossRef] [PubMed]
2. Carpenter, C.P.; Tolley, E.; Tourville, E.; Sharadin, C.; Giel, D.W.; Gleason, J.M. Hydronephrosis After Pyeloplasty: "Will It Go Away?". *Urology* **2018**, *121*, 158–163. [CrossRef] [PubMed]
3. Kaura, K.S.; Kumar, M.; Sokhal, A.K.; Gupta, A.K.; Purkait, B.; Saini, D.; Sankhwar, S. Giant Hydronephrosis: Still a Reality! *Turk. J. Urol.* **2017**, *43*, 337–344. [CrossRef] [PubMed]
4. Kwon, H.J.; Park, J. Missed Diagnosis of Giant Hydronephrosis Mimicking Abdominal Lymphatic Malformation or Omental Cyst in a 16-Year-Old Girl: A Case Report. *Int. J. Surg. Case Rep.* **2025**, *133*, 111533. [CrossRef] [PubMed]
5. Vali, R.; Armstrong, I.S.; Bar-Sever, Z.; Biassoni, L.; Borgwardt, L.; Brown, J.; Grant, F.D.; Mandell, G.A.; Majd, M.; Nadel, H.R.; et al. SNMMI Procedure Standard/EANM Practice Guideline on Pediatric [99mTc]Tc-DMSA Renal Cortical Scintigraphy: An Update. *Clin. Transl. Imaging* **2022**, *10*, 173–184. [CrossRef]
6. Grierosu, I.C.; Starcea, I.M.; Jalloul, W.; Mocanu, M.A.; Bogos, R.A.; Lazaruc, T.I.; Beldie, M.A.; Tibu, R.; Ionescu, T.M.; Stolniceanu, C.R.; et al. Particularities in the "Oldie but Goldie" Tc-99m DMSA Renography: A Retrospective Reference Centre Overview of 931 Children. *Diagnostics* **2025**, *15*, 1025. [CrossRef] [PubMed]
7. Chiriac, I.A.; Mititelu, R.M.; Mazilu, C.; Niculescu, O.; Lepus, M.G. Scintigraphic Evaluation of the Kidney. *Rom. J. Mil. Med.* **2015**, *118*, 26–32. [CrossRef]
8. Majd, M.; Bar-Sever, Z.; Santos, A.I.; De Palma, D. The SNMMI and EANM Procedural Guidelines for Diuresis Renography in Infants and Children. *J. Nucl. Med.* **2018**, *59*, 1636–1640. [CrossRef] [PubMed]
9. Piepsz, A.; Colarinha, P.; Gordon, I.; Hahn, K.; Olivier, P.; Roca, I.; Sixt, R.; van Velzen, J.; Paediatric Committee of the European Association of Nuclear Medicine. Guidelines for 99mTc-DMSA Scintigraphy in Children. *Eur. J. Nucl. Med.* **2001**, *28*, BP37–BP41. [PubMed]
10. Weyer, K.; Nielsen, R.; Petersen, S.V.; Christensen, E.I.; Rehling, M.; Birn, H. Renal Uptake of 99mTc-Dimercaptosuccinic Acid Is Dependent on Normal Proximal Tubule Receptor-Mediated Endocytosis. *J. Nucl. Med.* **2013**, *54*, 159–165. [CrossRef] [PubMed]
11. Schwartz, G.J.; Muñoz, A.; Schneider, M.F.; Mak, R.H.; Kaskel, F.; Warady, B.A.; Furth, S.L. New equations to estimate GFR in children with CKD. *J. Am. Soc. Nephrol.* **2009**, *20*, 629–637. [CrossRef] [PubMed]
12. Grandaliano, G.; Gesualdo, L.; Bartoli, F.; Ranieri, E.; Monno, R.; Leggio, A.; Paradies, G.; Caldarulo, E.; Infante, B.; Schena, F.P. MCP-1 and EGF Renal Expression and Urine Excretion in Human Congenital Obstructive Nephropathy. *Kidney Int.* **2000**, *58*, 182–192. [CrossRef] [PubMed]
13. Huang, W.-Y.; Peters, C.A.; Zurakowski, D.; Borer, J.G.; Diamond, D.A.; Bauer, S.B.; McLellan, D.L.; Rosen, S. Renal Biopsy in Congenital Ureteropelvic Junction Obstruction: Evidence for Parenchymal Maldevelopment. *Kidney Int.* **2006**, *69*, 137–143. [CrossRef] [PubMed]
14. Mankoff, D.A. A Definition of Molecular Imaging. *J. Nucl. Med.* **2007**, *48*, 18N–21N. [PubMed]
15. Lee, B.H.; Lee, S.H.; Choi, H.J.; Kang, H.G.; Oh, S.W.; Lee, D.S.; Ha, I.S.; Choi, Y.; Cheong, H.I. Decreased Renal Uptake of (99m)Tc-DMSA in Patients with Tubular Proteinuria. *Pediatr. Nephrol.* **2009**, *24*, 2211–2216. [CrossRef] [PubMed]
16. Nam, J.K.; Lee, S.D.; Chung, M.K. Modified Differential Renal Function Measurement Revised by Renal Cross Sectional Area in Children with Ureteropelvic Junction Obstruction. *Korean J. Urol.* **2010**, *51*, 271–275. [CrossRef] [PubMed]
17. Filippi, L.; Bagni, O.; Marcellino, A.; Lubrano, R. A Rare Case of a Pediatric Patient Affected by Crossed Fused Renal Ectopia: The Usefulness of Dual Tracer 99mTc-Diethylenetriamine Pentaacetic Acid/99mTc-Dimercaptosuccinic Acid Scintigraphy. *Indian J. Nucl. Med.* **2020**, *35*, 374–376. [CrossRef] [PubMed]
18. Woźniak, M.M.; Ključevšek, D.; Damasio, M.B.; Lobo, L.; Mentzel, H.-J.; Ording-Müller, L.-S.; Petit, P.; Riccabona, M.; Stafrace, S.; Smets, A.M.; et al. ESR Essentials: Renal Imaging in Children-Practice Recommendations by the European Society of Paediatric Radiology. *Eur. Radiol.* **2026**, *36*, 3611–3627. [CrossRef] [PubMed]
19. Pensabene, M.; Spataro, B.; Baldanza, F.; Grasso, F.; Serra, G.; Notarbartolo, V.; Giuffrè, M.; Corsello, G.; Zambaiti, E.; Di Pace, M.R.; et al. Application of Ultrasound in Primary Vesicoureteral Reflux: From Diagnosis to Follow Up. *Children* **2025**, *12*, 1363. [CrossRef] [PubMed]
20. Hemal, A.K.; Aron, M.; Wadhwa, S.N. Nephroplication and Nephropexy as an Adjunct to Primary Surgery in the Management of Giant Hydronephrosis. *Br. J. Urol.* **1998**, *81*, 673–677. [CrossRef] [PubMed]
21. Sarhan, O.; Al Otay, A.; Al Faddagh, A.; El Helaly, A.; Al Hagbani, M.; Al Ghanbar, M.; Al Kawai, F.; Nakshabandi, Z. Pyeloplasty in Children with Low Differential Renal Function: Functional Recoverability. *J. Pediatr. Urol.* **2021**, *17*, 658.e1–658.e9. [CrossRef] [PubMed]
22. Patil, S.R.; Pawar, P.W.; Savalia, A.J.; Mundhe, S.T.; Narwade, S.S.; Tamhankar, A.S. Role of calculated glomerular filtration rate using percutaneous nephrostomy creatinine clearance in the era of radionuclide scintigraphy. *Urol. Ann.* **2017**, *9*, 61–67. [CrossRef] [PubMed]

23. Chandrasekharam, V.V.S.; Shah, M.; Padua, M.; Babu, R.; Vittalraj, P.; Sundaram, S. Results of Temporary Drainage of Poorly Functioning Kidneys With Ureteropelvic Junction Obstruction: Does the Histology of Persistent Poor Functioning Kidneys Indicate an Increased Risk of Hypertension? *Urology* **2024**, *184*, 189–194. [CrossRef] [PubMed]
24. Menon, P.; Rao, K.L.N.; Bhattacharya, A.; Mittal, B.R. Outcome analysis of pediatric pyeloplasty in units with less than 20% differential renal function. *J. Pediatr. Urol.* **2016**, *12*, 171.e1–171.e7. [CrossRef] [PubMed]

Disclaimer/Publisher's Note: The statements, opinions and data contained in all publications are solely those of the individual author(s) and contributor(s) and not of MDPI and/or the editor(s). MDPI and/or the editor(s) disclaim responsibility for any injury to people or property resulting from any ideas, methods, instructions or products referred to in the content.